1. Introduction

Axles are connected within vehicles to perform two important functions: (i) they transmit torque from variance to wheel through planetary gear arrangement, and (ii) they maintain the position of the wheels comparative to each other and to the body of the vehicle. In most non-commercial vehicles, the circular motion of the drive wheels is maintained by means of axle shafts, which are integral component of the rear axle [1]. The shafts are installed in the tire's wheel well near the differentials and stretch across the bottom of the vehicle. Often during operation, the axle shafts are subjected to heavy torque due to loads or sudden acceleration and therefore, they are manufactured from different grades of hardened steels. There were four numbers of such axle shafts in service at the fork lift, out of which two failed. The fork lift is used to lift wire rod coils from the coil yard. An axle shaft of fork lift failed at operation within 296 h of service. No damage was reported in the other components of the assembly. Sudden jerk was observed before failure, which might be due to the effect of overloading. The fractured shaft with a diameter of about 7 cm was manufactured by the forging of 42CrMo4 grade of steel given an induction

hardening treatment to produce a case of 3–4 mm in depth as per specification. A section of fractured rear axle shaft was removed from the location to determine the most feasible cause of failure.

2. Experimental procedure

The failed axle shafts were collected from the plant for investigations. The samples were cleaned with acetone to remove dirt for visual examination prior to metallographic sample preparation. Transverse and longitudinal specimens were made from the fractured end of the failed samples for conducting optical microscopic examination. These samples were individually mounted in conductive mounting and polished by conventional metallographic techniques for scratch free surface. The polished samples were etched in 3% Nital solution (3 mL HNO_3 in 97 mL ethyl alcohol), and both un-etched and etched samples were examined under an optical microscope. The micro-hardness of different location which was observed in the failed samples was determined in a pneumatically controlled automatic micro hardness tester (Leco-$LM247_{AT}$). An applied load of 100 gf was used during testing, and several indentations were made to determine the hardness of the failed component. Field Emission Gun Scanning Electron Microscopy (FEG-SEM) of the samples was also carried out to identity exact phases present in the samples. The analyses were performed at 15 keV accelerating voltage and 5^{10-8} A probe current.

3. Results and discussions

3.1. Visual observation

Fig. 1a is a schematic illustration of the rear axle shaft showing the approximate location of the fracture near the wheel mounting flange. A photograph of the section received for analysis is shown in Fig. 1b. The axle shaft failed in shear mode at almost 45° to the longitudinal direction under torque [2,3]. It is observed that the fracture surface consists of two distinct regions: (i) a relatively smooth annular region at periphery marked as A where the fracture was initiated, and (ii) a rough core marked as B (shown in Fig. 1c).

3.2. Chemical analysis

The chemistry of the failed axle shaft matches with 42CrMo4 grade of steel. Chemical analyses of the failed sample are given in Table 1.

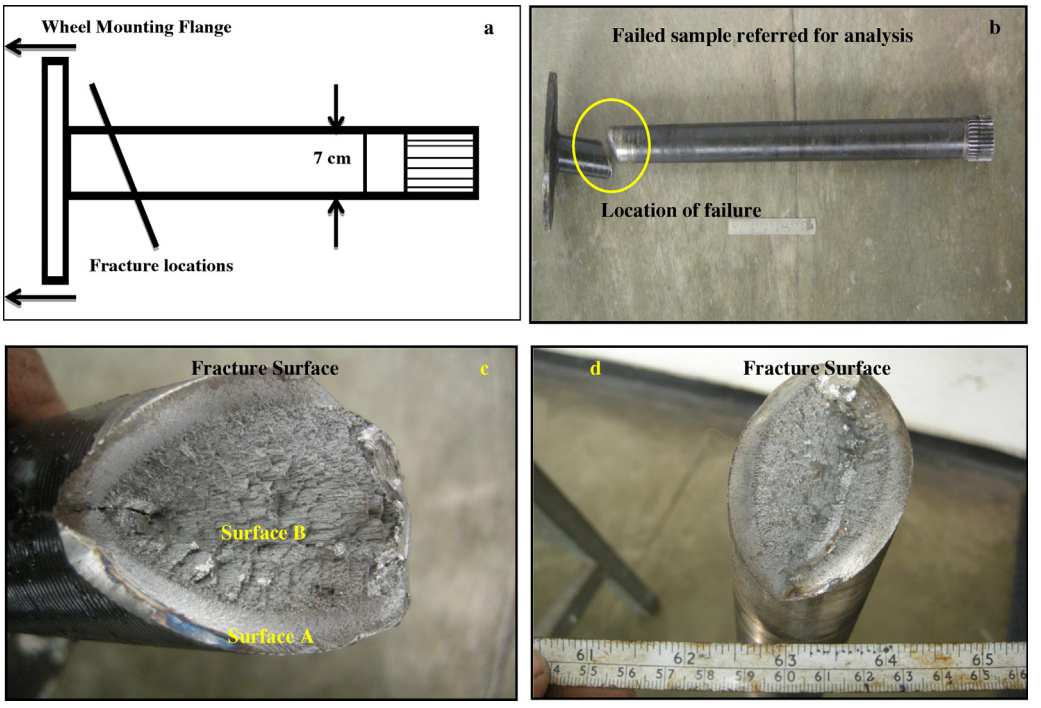

Fig. 1. (a) Schematic illustration of the rear axle shaft showing the approximate location of the fracture near the wheel mounting flange; (b) general view of the failed axle shaft referred for analysis; (c) closer view of the fracture surface of the failed component.

Table 1
Particulars of failed samples.

Sample type	C	Mn	S	P	Si	Cr	Mo	Dia. (cm)
Failed shaft	0.415	0.785	0.03	0.01	0.255	1.045	0.172	7.0
Specification (42CrMo4)	0.38–0.45	0.60–0.90	0.035 max	0.025 max	0.40	0.9–1.2	0.15–0.3	

3.3. Fractography

Fractography of the outer surface (region A) revealed cleavage nature of the fracture surface suggesting brittle fracture (Fig. 2a), whereas the fractography of the inner core (region B) revealed dimple nature of the fracture surface suggesting ductile fracture (Fig. 2b).

3.4. Microstructural analysis

The failed sample was etched with 2% Nital solution. The macrostructure at the cross-section of the rod reveals case hardened layer as the component was subjected to induction hardening treatment (Fig. 3a). The hardening layer was non-uniform along the cross-section and in some location it was found more than the specification (>2–3 mm). The un-etched microstructure reveals numerous sulphide inclusions throughout the sample which indicates that the steel is not clean (Fig. 3b). The surface of the rod sample reveals in-homogeneous/banded microstructure in martensitic matrix (Fig. 3c), whereas the core reveals ferrite pearlite structure (Figs. 3b). Mixture of coarse and fine pearlite structure was observed in the core of the sample which was resulted due to improper heat treatment process.

3.5. Inclusion rating

Inclusion rating of the failed component was carried out as per ASTM E-45. Un-etched microstructure of shaft shows that thin and thick sulphide (Type A) inclusions are present with a severity of 2.5 and 0.5 respectively. Some inclusions of Type D (oxides) are observed with a severity of 0.5. Such a huge number of inclusions are not desirable as they can act as stress concentration sites and may lead to crack initiation (as shown in Table 2).

3.6. FEG-SEM analysis

Non-metallic inclusions were observed along the longitudinal axis of the component. Elemental analysis under SEM reveals that the inclusions were found to be rich in Sulphur (S) and Manganese (Mn) indicating them to be manganese sulphide inclusions (as shown in Table 3). The crack in this region has propagated by brittle mode and MnS inclusions could have enhanced the notch sensitivity of the shaft [4–6] (Fig. 4).

3.7. Hardness profile

Non-uniform distribution of hardness was observed in the rod sample across the section (Fig. 5). The average hardness of the surface hardened layer is measured to be 735 HV which is very high compared to the core and also for these applications. Such high hardness is not desirable since it imparts brittleness.

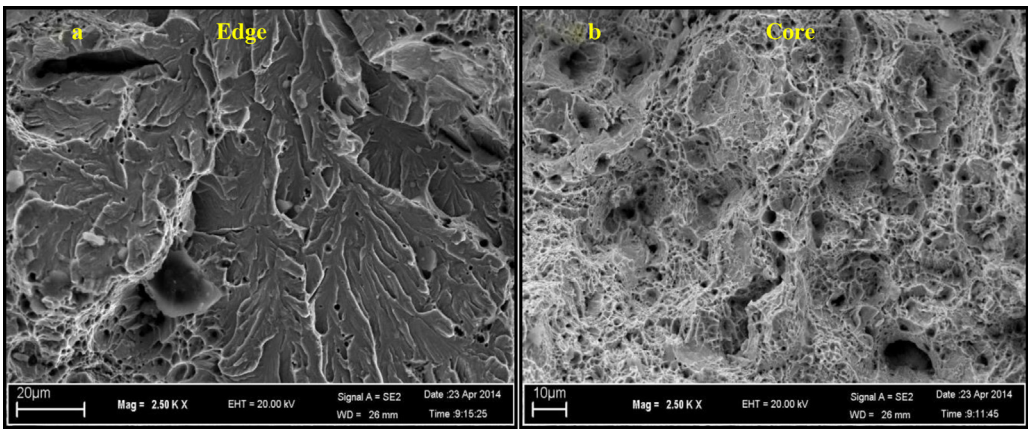

Fig. 2. (a) Fractography analysis of side A of the failed component; (b) fractography analysis of side B of the failed component.

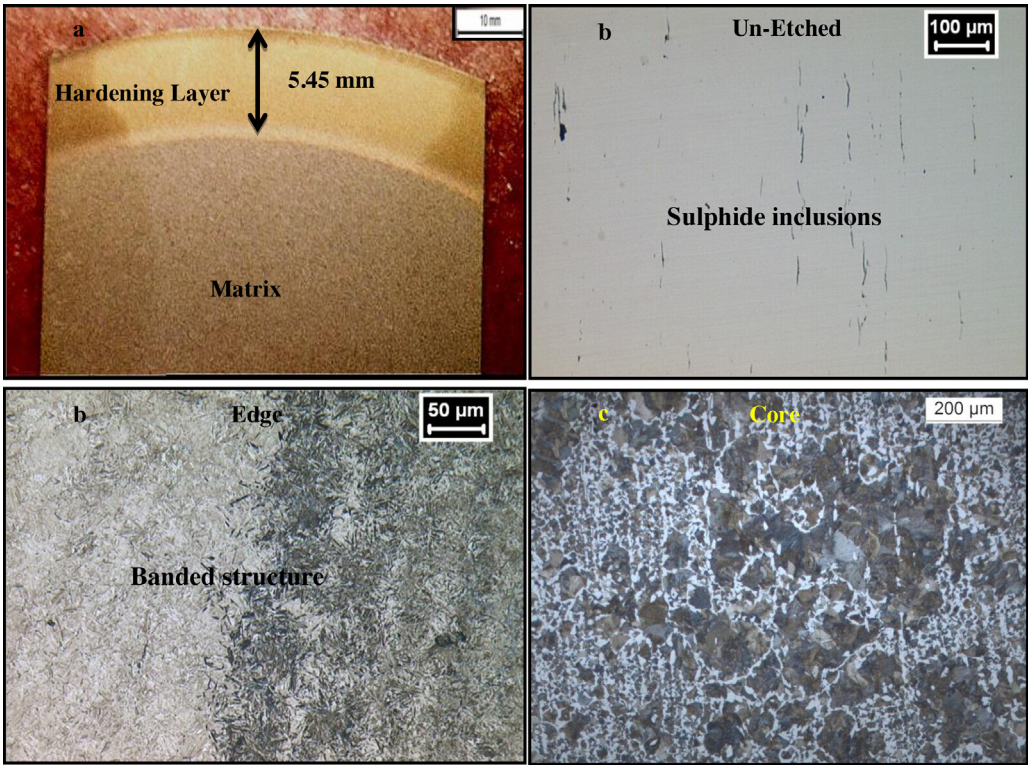

Fig. 3. (a) Macrostructure of the cross-section of the failed shaft; (b) un-etched structure of the failed shaft; (c) microstructure of the edge of the component; (d) microstructure of the edge of the component.

4. Discussions

The fork lift is used to lift wire rod coils from the coil yard. No damage was reported in other components of the assembly. The fractured shaft with a diameter of about 7 cm was manufactured by forging of 42CrMo4 grade of steel given an induction hardening treatment to be producing a case of 3–4 mm in depth as per specification. A section of fractured rear axle shaft removed from the location was received to determine the most feasible cause of failure. The axle shaft failed on shear mode at 45° to the longitudinal direction under torque. It is observed that the fracture surface consists of two distinct regions: (i) a relatively smooth annular region at periphery marked as A where the fracture was initiated, and (ii) a rough core marked as B. Fractography of the outer surface (region A) revealed cleavage nature of the fracture surface suggesting brittle fracture, whereas the fractography of the inner core (region B) revealed dimple nature of the fracture surface suggesting ductile fracture The macrostructure at the cross-section of the rod reveals case hardened layer as the component was subjected to induction hardening treatment. The hardening layer was non-uniform along the cross-section and in some location it was found more than the specification (>2–3 mm). The un-etched microstructure reveals numerous sulphide inclusions

Table 2
Inclusion rating.

Sample	A (thin/heavy)	B (thin/heavy)	C (thin/heavy)	D (thin/heavy)
Axle shaft	2.5/0.5	0.0/0.0	0.0/0.0	0.5/0.0

Table 3
EDS analysis (wt.%).

Spectrum	S	Mn	Total
1	37.83	62.17	100.00
2	38.62	61.38	100.00

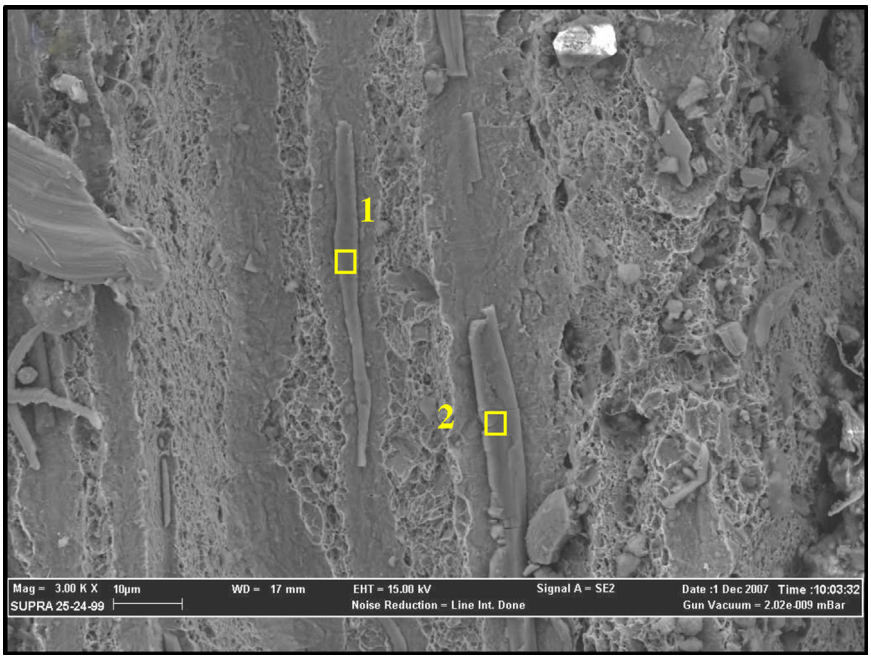

Fig. 4. The fracture surface shows multiple sulphide stringers oriented in the direction of crack propagation.

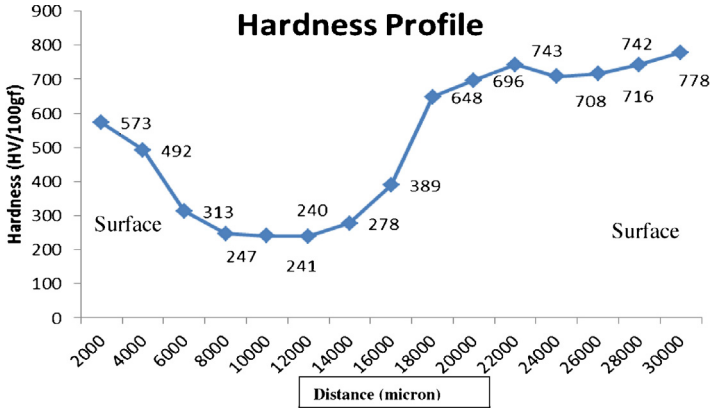

Fig.5. The hardness profile of the transverse section of the shaft.

throughout the sample which indicates that the steel is not clean. The surface of the rod sample reveals in-homogeneous/banded microstructure in martensitic matrix, whereas the core reveals ferrite pearlite structure. Mixture of coarse and fine pearlite structure was observed in the core of the sample which was resulted due to improper heat treatment process. The difference in fracture behaviour is caused by variation in microstructure of the case and core resulting from the improper hardening treatment. Due to improper heat treatment of the shaft which is resulting in case microstructure with poor ductility due to high hardness which results in the material more susceptible to brittle fracture. Non-metallic inclusions were observed along the longitudinal axis of the component. Elemental analysis under SEM reveals that the inclusions were found to be rich in Sulphur (S) and Manganese (Mn) indicating them to be manganese sulphide inclusions (as shown in Table 3). The crack in this region has propagated by brittle mode and MnS inclusions could have enhanced the notch sensitivity of the shaft.